Original Article
Diagnostic efficacy of C-X-C motif chemokine receptor 4-directed PET/CT in newly diagnosed head and neck squamous cell carcinoma - a head-to-head comparison with [18F]FDG

Yingjun Zhi[1], Rudolf A Werner[2,3], Andreas Schirbel[2], Takahiro Higuchi[2,4], Andreas K Buck[2], Aleksander Kosmala[2], Thorsten A Bley[5], Rudolf Hagen[1], Stephan Hackenberg[6], Andreas Rosenwald[7], Agmal Scherzad[1], Elena Gerhard-Hartmann[7*], Sebastian E Serfling[2*]

[1]Department of Otorhinolaryngology, Plastic, Aesthetic and Reconstructive Head and Neck Surgery, University Hospital Würzburg, Würzburg 97080, Germany; [2]Department of Nuclear Medicine, University Hospital Würzburg, Würzburg 97080, Germany; [3]Division of Nuclear Medicine, The Russell H. Morgan Department of Radiology and Radiological Science, Johns Hopkins University School of Medicine, Baltimore, MD 21205, USA; [4]Faculty of Medicine, Dentistry and Pharmaceutical Sciences, Okayama University, Okayama 700-8530, Japan; [5]Department of Diagnostic and Interventional Radiology, University Hospital Würzburg, Würzburg 97080, Germany; [6]Department of Otorhinolaryngology - Head and Neck Surgery, RWTH Aachen University, Aachen 52074, Germany; [7]Department of Pathology and Comprehensive Cancer Center Mainfranken, Julius-Maximilian University of Würzburg, Würzburg 97080, Germany. *Equal contributors.

Abstract: Background: The aim of this study was to determine the read-out capabilities of the novel C-X-C motif chemokine receptor 4 (CXCR4)-targeting radiotracer [68Ga]Ga-PentixaFor compared to the reference radiotracer [18F]FDG in untreated individuals with head and neck squamous cell carcinoma (HNSCC). Material and Methods: 12 patients with histologically confirmed HNSCC were scheduled for [18F]FDG and [68Ga]Ga-PentixaFor PET/CT. Maximum standardized uptake values (SUV_{max}) and target-to-background ratios (TBR) were applied with vena cava superior serving as reference. In addition, we compared [68Ga]Ga-PentixaFor-PET findings with immunohistochemical (IHC) results of CXCR4 expression. Results: On visual assessment, [18F]FDG identified more sites of disease, with increased detection rates for both the primary tumor ([18F]FDG, 12/12 [100%] vs. [68Ga]Ga-PentixaFor, 10/12 [83%]) and LN metastases ([18F]FDG, 9/12 [75%] vs. [68Ga]Ga-PentixaFor, 8/12 [67%]). Indicative for improved image contrast using [18F]FDG, quantification showed a higher TBR for the latter radiotracer, when compared to [68Ga]Ga-PentixaFor for all lesions ([18F]FDG, 11.7 ± 8.5 vs. [68Ga]Ga-PentixaFor, 4.3 ± 1.3; P=0.03), primary tumors ([18F]FDG, 13.6 ± 8.7 vs. [68Ga]Ga-PentixaFor, 4.4 ± 1.4; P<0.01), and LN lesions ([18F]FDG, 9.3 ± 10.6 vs. [68Ga]Ga-PentixaFor, 4.7 ± 1.5; P=0.3). IHC showed variable CXCR4 expression in the primary and LN, along with no associations between ex-vivo CXCR4 upregulation and [68Ga]Ga-PentixaFor-based TBR (R=0.33, P=0.39) or SUV_{max} (R=0.44, P=0.2). Of note, IHC also revealed heterogeneous expression of CXCR4 in immune cells in the tumor microenvironment and in germinal centers, indicative for inflammatory reactions. Conclusions: In HNSCC, [18F]FDG demonstrated superior diagnostic performance relative to [68Ga]Ga-PentixaFor, in particular for assessment of the primary. Based on the IHC analyses, these findings may be explained by CXCR4 upregulation not only by tumor but also by immune cells in the tumor microenvironment.

Keywords: PET, PET/CT, CXCR4, HSNCC, head and neck squamous cell carcinoma, [68Ga]Ga-PentixaFor

Introduction

Head and neck squamous cell carcinoma (HNSCC) is a devastating disease with a high mortality rate [1]. Despite advances in diagnosis and treatment, overall survival (OS) remains poor [1] and outcome is associated with tumor localization, size of the primary and number of metastases [2]. However, with the recent introduction of immune checkpoint inhibitors, outcome improvements have been achieved in the palliative setting while also neoadjuvant clinical

Table 1. Patient's characteristics

Patient no.	Age	Smoker	Tumor localisation
#1	52	Y	Hypopharynx
#2	35	N	Edge of the tongue
#3	62	Y	Oropharynx
#4	71	Y	Tonsil
#5	60	Y	Tongue
#6	62	Y	Larynx
#7	84	Y	Larynx
#8	67	Y	Larynx
#9	71	Y	Hypopharynx
#10	59	Y	Base of tongue
#11	72	Y	Larynx
#12	56	Y	Base of tongue

trials show promising results [3]. Early detection and accurate staging of these tumors are essential to optimize treatment and improve therapy outcome [4]. PET/CT is a widely used imaging modality for HNSCC staging and in this regard, [18F]FDG is the current radiotracer of choice [5]. However, despite its widespread use, this positron-emitting agent has several limitations, e.g., for reliable detection of small tumors, and differentiation between tumor recurrence and post-treatment changes [6, 7]. Among others, chronic inflammation in the oro-nasopharyngeal cavity can cause false positive results on [18F]FDG PET [8]. Furthermore, the primary tumor may appear larger on imaging, most commonly due to ulceration and associated inflammation [9]. Moreover, inflammatory changes can lead to reactive lymphadenopathy that may mimic lymphatic tumor spread [10]. Thus, accurate delineation of the primary tumor is often not feasible with [18F]FDG, since the used glucose analog also accumulates in inflammatory changes in the primary tumor or regional lymph nodes (LN) [11]. C-X-C motif chemokine receptor 4 (CXCR4), a transmembrane G-protein receptor, is known to be over-expressed in HNSCC. Previously, it has been reported that the upregulation of CXCR4 in tumor cells - determined by immunohistochemistry (IHC) - indicates a prognostic factor in patients with HNSCC. These patients may have higher rates of LN metastasis [12] and a higher association with recurrence [13].

We aimed to compare the performance of CXCR4-directed PET/CT with the reference radiotracer [18F]FDG for staging of HNSCC, also focusing on comparison of the [68Ga]Ga-PentixaFor PET signal with histopathologic results.

Material and methods

General

As this was a retrospective study, the local ethics committee of the University Hospital Würzburg waived the need for further approval (waiver No.: 20210726 02). Informed consent for diagnostic procedures was obtained from all included subjects. 12 male patients between 35-84 years (62.6 ± 12.3 y) with a histologically confirmed HNSCC were investigated (**Table 1**).

Radiotracer synthesis

[68Ga]Ga-PentixaFor was prepared using a Scintomics synthesis module (Scintomics, Fürstenfeldbruck, Germany). In this automated variant, sterile disposable cassette units from ABX (Radeberg, Germany) are used to enable GMP-compliant synthesis [14]. Quality control was also conducted. [18F]FDG was also produced by automated synthesis on a FastLab module under GMP conditions. For this purpose, [18F]fluoride was applied, which was previously obtained in our in-house cyclotron (GE 800).

Imaging procedures and analysis

All patients underwent imaging with [18F]FDG using a mean activity of 228 ± 43 MBq. Iodine-containing contrast medium was also applied to allow for potential preoperative planning [15]. 60 minutes after injection, imaging (whole body, skull to mid-thigh) was performed using a Siemens Biograph mCT 128 (Siemens Healthineers, Erlangen, Germany). Within one week, all patients received an additional CXCR4-directed PET with low-dose CT after administration of 141 ± 22 MBq [68Ga]Ga-PentixaFor (without treatment between scans). All PET images were reconstructed iteratively in accordance with the manufacturer's implementation (Siemens Healthineers, Erlangen, Germany) [15]. A 3D mode (200×200 matrix, 3 iterations, minimum 21 subsets, Gaussian filtering 2 mm) was used. Reference tube current was 35 mAs (low-dose scans; 160 mAs, full dose scans; minimum 100 keV tube voltage;

minimum 0.8 pitch; rotation time of 0.5 sec). 3.0-5.0 mm slices were applied for the CT imaging procedure [16]. Evaluation of CT, CXCR4-directed PET and hybrid imaging was performed by an expert reader (S.E.S.). The quantification on both [18F]FDG and [68Ga]Ga-PentixaFor PET was carried out as follows: Volume of interest (VOI) were placed over target lesions (TL) in disease sites, providing maximum standardized uptake values (SUV_{max}), which were then compared between both radiotracers. Moreover, mean standardized uptake values (SUV_{mean}) were also determined by using VOIs over vena cava superior (VCS). The respective target-to-background ratio (TBR) was defined to provide a quantitative read-out of image contrast and to compare TBR between [68Ga]Ga-PentixaFor vs. [18F]FDG:

$$TBR = SUV_{max} (TL)/SUV_{mean\_VCS} \qquad Eq.\ 1.$$

Histology and immunohistochemistry (IHC)

Sections were cut and stained with hematoxylin and eosin for routine histologic evaluation. CXCR4 IHC was performed in the primary tumors and available LNs, and CXCR4 expression investigated in tumor cells and surrounding immune cells. CXCR4 IHC (antibody 124824, Abcam, Cambridge, UK; dilution 1:1000) was carried out on formalin-fixed paraffin-embedded tissue slides using a Leica autostainer (Wetzlar, Germany) according to the manufacturers' instructions and standard protocols. Nuclear contrast was achieved by hematoxylin counterstaining.

CXCR4 immunostaining was classified using the H-Score (HS) [17]. Briefly, staining intensity and percentage of positive cells were evaluated and summed as follows:

1× (% weakly positive cells 1) + 2× (% moderately positive cells 2) + 3× (% strongly positive cells 3)   *Eq. 2,*

giving a range of 0 to 300. Respective HS were then compared with [68Ga]Ga-PentixaFor PET-derived SUV_{max} and TBR.

Statistical analysis

GraphPad Prism (9.3, GraphPad Software, San Diego, CA) was used. Quantitative results are presented as mean and standard deviation. Paired Student's t-test and linear regression analyses were applied. A *p* value of 0.05 indicated statistical significance.

Results

[68Ga]Ga-PentixaFor is inferior to [18F]FDG on a visual and quantitative assessment

On a patient-based assessment, [18F]FDG identified more disease sites, with increased detection rates for both the primary tumor ([18F]FDG, 12/12 [100%], [68Ga]Ga-PentixaFor, 10/12 [83%]) and LN metastases ([18F]FDG, 9/12 [75%], [68Ga]Ga-PentixaFor, 8/12 [67%]).

Quantification yielded the following results: higher TBR were observed for [18F]FDG when compared to [68Ga]Ga-PentixaFor for all lesions ([18F]FDG, 11.7 ± 8.5 vs. [68Ga]Ga-PentixaFor, 4.3 ± 1.3; P=0.03), primary ([18F]FDG, 13.6 ± 8.7 vs. [68Ga]Ga-PentixaFor, 4.4 ± 1.4; P<0.01) and LN ([18F]FDG, 9.3 ± 10.6 vs. [68Ga]Ga-PentixaFor, 4.7 ± 1.5; P=0.3). Following results were observed for SUV_{max}: all lesions, [18F]FDG, 19.1 ± 8.1 vs. [68Ga]Ga-PentixaFor, 7.8 ± 2.4 (P<0.01); primary, [18F]FDG, 23.0 ± 9.6 vs. [68Ga]Ga-PentixaFor, 8.0 ± 2.9 (P<0.001); and LN, [18F]FDG, 13.8 ± 9.84 vs. [68Ga]Ga-PentixaFor, 8.3 ± 2.3 (P=0.3).

Figure 1 shows a patient with carcinoma of the base of the tongue with a histologically confirmed LN metastasis of the right side, which was correctly identified on [18F]FDG. Further findings in cervical LNs on both sides, however, were exclusively detected by [68Ga]Ga-PentixaFor. Upon histological work-up, however, these LNs turned out to be inflammatory/reactive changes with lymphofollicular hyperplasia, also indicating that chemokine receptor PET may provide false-positive findings.
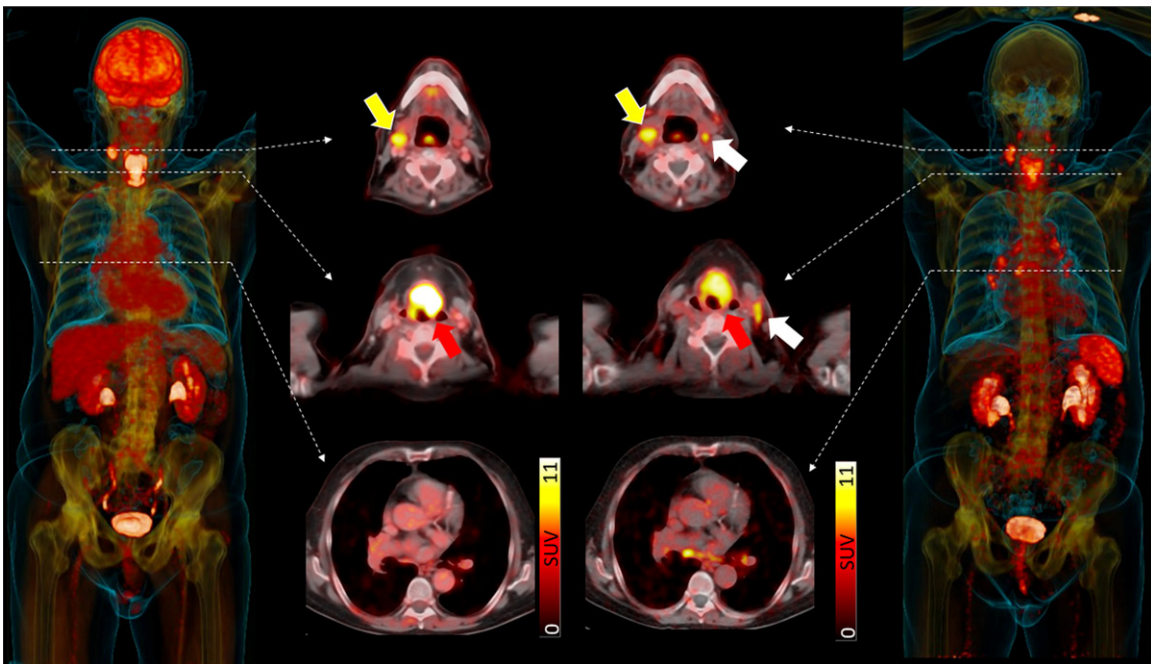
Figure 2 displays a patient with larynx carcinoma and [18F]FDG provided improved diagnostic capability in identifying both the primary and LN metastasis. Again, moderate uptake on contralateral cervical LN on CXCR4-targeted PET/CT were considered false-negative when compared to IHC.

IHC shows heterogeneous CXCR4 expression and no relevant association with [68Ga]Ga-PentixaFor PET signal

In 9/12 (75%), available specimens from the primary tumor were sufficient for further histo-
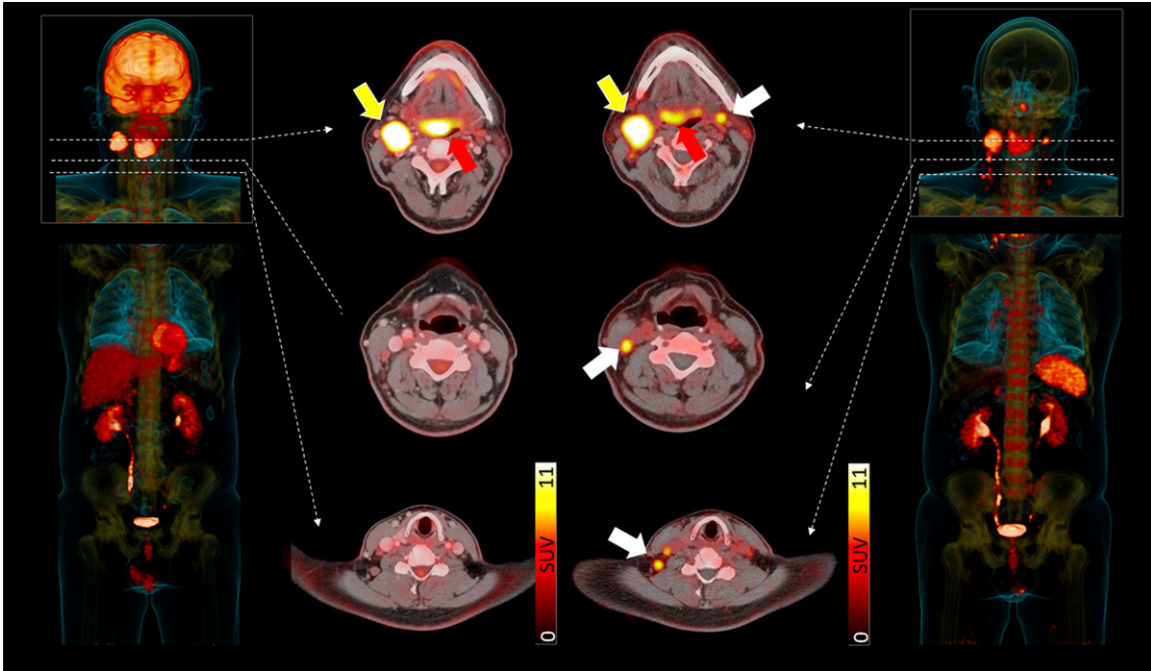
Figure 1. Patient #12 with carcinoma of the base of the tongue (red arrow) with a histologically confirmed lymph node (LN) metastasis of the right side (yellow arrow) on [18F]FDG PET/CT. Further findings in cervical LN regions (white arrows), however, were exclusively detected by [18F]FDG-directed [68Ga]Ga-PentixaFor PET/CT. The maximum intensity projection (MIP) of a [18F]FDG PET/CT is shown on the left (right, MIP of [68Ga]Ga-PentixaFor PET/CT). In the middle, three transaxial PET/CT images for [18F]FDG (left) and [68Ga]Ga-PentixaFor PET/CT (right) are also displayed. In addition to the primary carcinoma exhibiting higher uptake on [18F]FDG relative to [68Ga]Ga-PentixaFor (red arrow), [18F]FDG identified a single LN metastasis in the right jaw angle (yellow arrow), which was also histologically confirmed. On [68Ga]Ga-PentixaFor PET/CT, several CXCR4 positive LN along the vascular nerve sheath on both cervical sides were identified, suggestive for LN metastases. Upon histological work-up, however, these LNs (white arrows) turned out to be inflammatory/reactive changes with lymphofollicular hyperplasia.

Figure 2. Improved detection for [18F]FDG relative to [68Ga]Ga-PentixaFor for both the primary (red arrows) and one lymph node metastasis (LN, yellow arrows) in a patient with larynx carcinoma. The maximum intensity projection

(MIP) of a [18F]FDG PET/CT is shown on the left (right, MIP of [68Ga]Ga-PentixaFor PET). The primary and a prominent right cervical LN metastasis is more clearly visible on the MIP of [^{18}F]FDG PET when compared to [^{68}Ga]Ga-PentixaFor MIP. Moreover, on transaxial PET/CT slides displayed in the middle, the contours of the primary appears more sharp on [^{18}F]FDG. CXCR4-avid LNs only seen on [^{68}Ga]Ga-PentixaFor on the MIP and transaxial PET/CTs (top, cervical LN right) turned out to be false-negative when compared to histopathological work-up (white arrows). There are also mediastinal LNs displayed on [^{68}Ga]Ga-PentixaFor PET which were not visible on [^{18}F]FDG. Upon follow-up, those LNs remained unchanged, indicative for inflammatory reaction at time of dual-radiotracer imaging.

logical workup. CXCR4 IHC showed a membranous and cytoplasmic staining in tumor cells. CXCR4 expression of tumor cells in the primary tumors was overall relatively modest, but variable (HS 48.1 ± 39.5; range, 4.0-120.0).

In the 4 histologically proven LN metastases available for CXCR4 IHC, a wider CXCR4 expression range of the tumor cells was observed (HS 110.5 ± 122.1; range, 5.0-275), which was mainly triggered by CXCR4 expression in the LN metastasis of patient #12.

Figure 3 displays respective immunohistochemical stainings of two individuals with high (patient no. #4; Figure 3A, 3B) vs. low (patient no. #12; Figure 3C, 3D) CXCR4 expression in the primary tumor, while for LN metastases, opposite findings were recorded (patient no. #4; Figure 3E, 3F low vs. patient no. #12; Figure 3G, 3H high CXCR4 expression). A high CXCR4 expression was also found in the germinal centers (GC, white arrows in Figure 3F, 3H) of the LN which in some cases was higher than in the tumor infiltrates (black arrows). Relative to those ex-vivo findings, quantified [^{68}Ga]Ga-PentixaFor-PET signal in those 2 patients (#4, #12) did not show such a variance, including the primaries and LN (range, 9.0-12.0 for SUV$_{max}$).

A comparable trend was then also observed for the entire cohort: When investigating the IHC-based CXCR4 HS with the [^{68}Ga]Ga-PentixaFor PET signal from all available primaries, no relevant associations between in- and ex-vivo findings was found (TBR, R=0.33, P=0.39; SUV$_{max}$, R=0.44, P=0.2). For LN, such an analysis was not conducted due to the low number of available LN specimen.

Discussion

In the present head-to-head comparison of [^{68}Ga]Ga-PentixaFor vs. [^{18}F]FDG PET/CT in patients with untreated HNSCC, the latter radiotracer provided superior image contrast in particular for the primary, along with no relevant associations between ex- and in-vivo CXCR4 expression levels. Our IHC results, however, indicate that these results may be explained by reactive/inflammatory conditions with increased CXCR4 expression of immune cells in the tumor microenvironment.

The PET Neck trial yielded favorable results for the use of [^{18}F]FDG in the setting of stage N2/3 HNSCC after primary radiochemotherapy. While such an image-guided treatment approach did not prolong survival, a substantial rate of surgical procedures were avoided, along with improved cost efficacy for patients randomized in the molecular imaging arm [18, 19]. Nonetheless, [^{18}F]FDG has multiple drawbacks, including its high background activity in the oral cavity, which hampers precise read-out or provides false-positive findings, e.g., due to chronic inflammation also causing a substantially increased PET signal in cervical LN [20]. Therefore, in recent years, novel radiotracers have been increasingly used to overcome these limitations. Among others, fibroblast activation protein inhibitor (FAPI)-targeting agents, such as [^{68}Ga]Ga-FAPI04 identified [^{18}F]FDG(-) primaries in patients affected with cancers of unknown primary most likely located in the head-neck region [21]. In addition, an increased FAP expression revealed by PET may also guide towards cancer-associated fibroblasts-targeting radioligand therapy [22].

Beyond targeting cancer-associated fibroblasts, such a theranostic "twin" is also available for another highly overexpressed molecular target in HNSCC, namely CXCR4. Of note, this chemokine receptor subtype has already been advocated to have prognostic value in this patient population [23]. Although the referring CXCR4-directed PET agent [^{68}Ga]Ga-PentixaFor has been primarily investigated for hematologic neoplasms, a recent overview of 690 patients also yielded relevant in-vivo chemokine receptor upregulation in solid tumors [24]. As such, it was the aim to compare
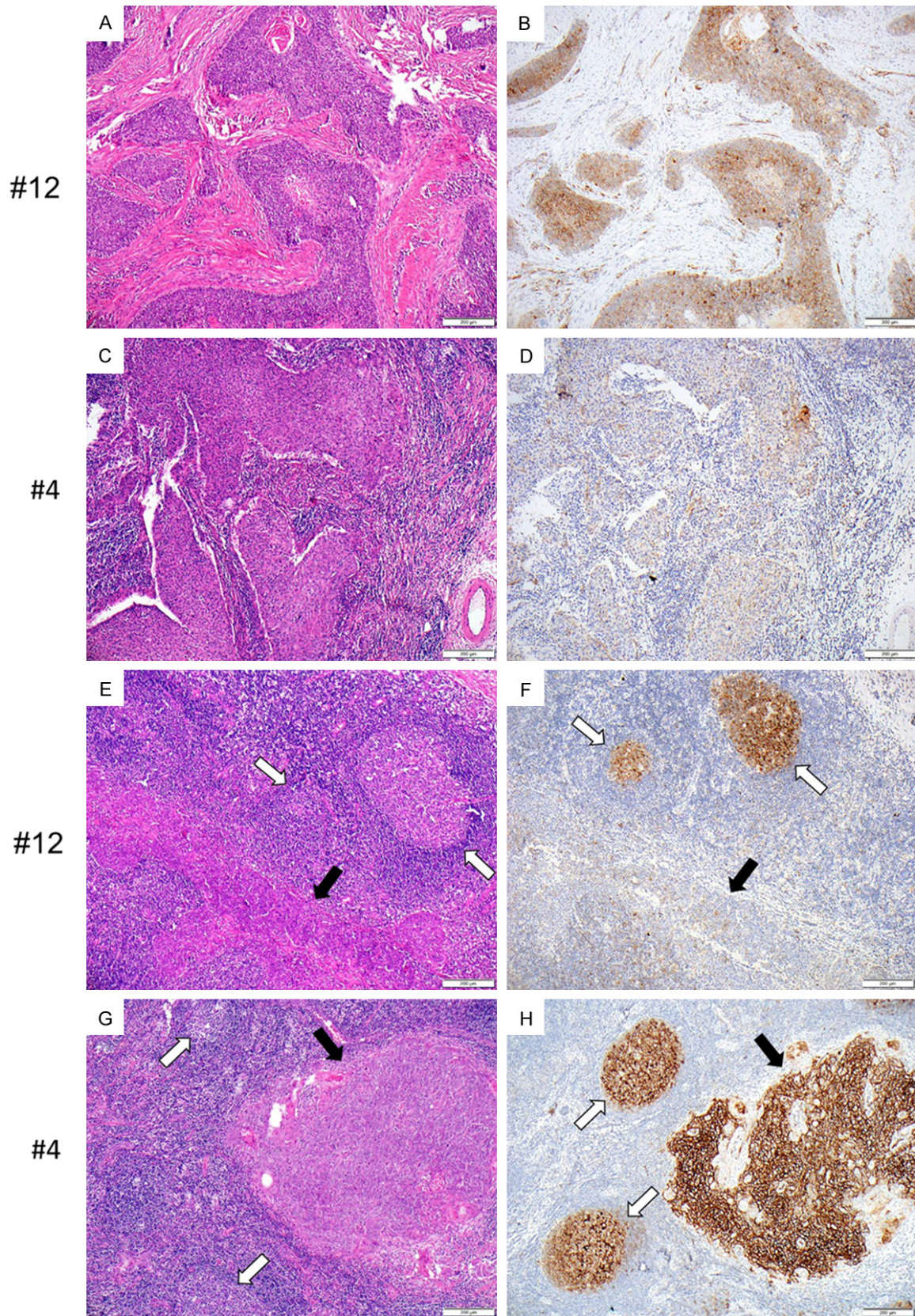
Figure 3. Immunohistochemistry (IHC) shows intra- and intertumoral variability of CXCR4 protein expression of the carcinoma cells. Haematoxylin and eosin (HE) (A) and CXCR4 IHC staining of the primary (B) and LN metastasis (E, F) of patient #12 and patient #4 (primary, HE: C; CXCR4: D; LN metastasis: G, H). A variable CXCR4 expression of

the tumor cells when comparing the primary tumor and LN metastasis was observed: For patient #12, CXCR4 expression was relatively high in the primary (B), but low in the LN metastasis (F, black arrows; HE control displayed in E). The primary tumor of patient #4 shows a relatively weak CXCR4 expression (D), but strong expression in the LN metastasis (H, black arrows; HE control displayed in G). However, in LN from both patients, lymphofollicular hyperplasia with prominent CXCR4 expression of the germinal centers of the lymph follicles was noted (F, H, white arrows; HE controls displayed in E, G), which indicates inflammatory reaction. Such a large variance of CXCR4 expression, however, was not observed on [^{68}Ga]Ga-PentixaFor PET in those two patients (range, 9.0-12.0 for SUV$_{max}$). All stainings are displayed by 10× objective; length of the scale bar is 200 μm.

the current reference radiotracer [^{18}F]FDG with the CXCR4-directed PET agent [^{68}Ga]Ga-PentixaFor in patients with newly diagnosed HNSCC, thereby allowing to determine the diagnostic capability of CXCR4 PET for staging in this patient group. However, the detection rate was lower for [^{68}Ga]Ga-PentixaFor compared to [^{18}F]FDG on a visual and quantitative assessment. Moreover, we also investigated CXCR4 expression on the primary and compared respective in-vivo (TBR, SUV$_{max}$) and ex-vivo findings (HS). No relevant associations were recorded and the overall limited performance of [^{68}Ga]Ga-PentixaFor may be partially explained by reactive/inflammatory conditions of the lymphoid tissue, e.g., lymphofollicular hyperplasia or immune cells in the tumor microenvironment. In our ex-vivo analysis, we also observed that CXCR4 is expressed in germinal center centroblasts, which was in some cases even higher than in tumor cells, indicative for inflammatory reactions in the tumor microenvironment [25, 26]. Taken together, although [^{18}F]FDG is associated with a high false positive rate due to inflammatory LN [27], [^{68}Ga]Ga-PentixaFor may rather also not overcome this issue and thus, even more specific, tumor-targeting radiotracers in the context of HNSCC are needed.

Last, CXCR4-directed radioligand therapies based on [^{68}Ga]Ga-PentixaFor PET may be used with caution, as use of its theranostic counterpart [^{90}Y]Y-PentixaTher was associated with (desired) myeloablation in hematologic neoplasm to prepare for stem cell transplantation [28]. This bone marrow eradication, however, would be a major side effect in patients with HNSCC and would also require stem cell backup, which may be harvested prior to treatment on-set in a salvage setting [29].

This study has limitations, including the small sample size, the limited number of available LN specimen for IHC and the retrospective nature of this investigation. Nonetheless, our preliminary findings may not favor a more widespread use of [^{68}Ga]Ga-PentixaFor for HNSCC and further studies are needed to determine the role of this theranostic agent in the clinic.

Conclusions

In HNSCC, [^{68}Ga]Ga-PentixaFor was inferior to [^{18}F]FDG on a visual and quantitative evaluation, along with no relevant associations of the [^{68}Ga]Ga-PentixaFor PET signal in the primary with ex-vivo CXCR4 expression. IHC also revealed heterogeneous expression of CXCR4 in immune cells in the tumor microenvironment and in germinal centers, indicative for inflammatory reactions, thereby explaining the limited performance of [^{68}Ga]Ga-PentixaFor in this patient population.

Disclosure of conflict of interest

R.A.W. has received speaker honoraria from PentixaPharm and is involved in [^{68}Ga]Ga-Pentixafor PET Imaging in PAN Cancer (FORPAN), sponsored and planned by PentixaPharm.

Address correspondence to: Dr. Sebastian E Serfling, Department of Nuclear Medicine, University Hospital Würzburg, No. 6 Oberdürrbacher Street, Würzburg 97080, Germany. Tel: +49-931-201-35001; E-mail: serfling_s1@ukw.de

References

[1] Kligerman MP, Sethi RKV, Kozin ED, Gray ST and Shrime MG. Morbidity and mortality among patients with head and neck cancer in the emergency department: a national perspective. Head Neck 2019; 41: 1007-15.

[2] Duprez F, Berwouts D, De Neve W, Bonte K, Boterberg T, Deron P, Huvenne W, Rottey S and Mareel M. Distant metastases in head and neck cancer. Head Neck 2017; 39: 1733-43.

[3]   Burtness B, Harrington KJ, Greil R, Soulieres D, Tahara M, de Castro G Jr, Psyrri A, Basté N, Neupane P, Bratland Å, Fuereder T, Hughes BGM, Mesía R, Ngamphaiboon N, Rordorf T, Wan Ishak WZ, Hong RL, González Mendoza R, Roy A, Zhang Y, Gumuscu B, Cheng JD, Jin F and Rischin D; KEYNOTE-048 Investigators. Pembrolizumab alone or with chemotherapy versus cetuximab with chemotherapy for recurrent or metastatic squamous cell carcinoma of the head and neck (KEYNOTE-048): a randomised, open-label, phase 3 study. Lancet 2019; 394: 1915-28.

[4]   Abramyuk A, Appold S, Zophel K, Baumann M and Abolmaali N. Modification of staging and treatment of head and neck cancer by FDG-PET/CT prior to radiotherapy. Strahlenther Onkol 2013; 189: 197-201.

[5]   Goel R, Moore W, Sumer B, Khan S, Sher D and Subramaniam RM. Clinical practice in PET/CT for the management of head and neck squamous cell cancer. AJR Am J Roentgenol 2017; 209: 289-303.

[6]   Hanamoto A, Takenaka Y, Shimosegawa E, Ymamamoto Y, Yoshii T, Nakahara S, Hatazawa J and Inohara H. Limitation of 2-deoxy-2-[F-18] fluoro-D-glucose positron emission tomography (FDG-PET) to detect early synchronous primary cancers in patients with untreated head and neck squamous cell cancer. Ann Nucl Med 2013; 27: 880-5.

[7]   Zschaeck S, Zophel K, Seidlitz A, Zips D, Kotzerke J, Baumann M, Troost EGC, Löck S and Krause M. Generation of biological hypotheses by functional imaging links tumor hypoxia to radiation induced tissue inflammation/glucose uptake in head and neck cancer. Radiother Oncol 2021; 155: 204-11.

[8]   Rusthoven KE, Koshy M and Paulino AC. The role of fluorodeoxyglucose positron emission tomography in cervical lymph node metastases from an unknown primary tumor. Cancer 2004; 101: 2641-9.

[9]   Bonomi M, Patsias A, Posner M and Sikora A. The role of inflammation in head and neck cancer. Adv Exp Med Biol 2014; 816: 107-27.

[10]   Di Martino E, Nowak B, Krombach GA, Sellhaus B, Hausmann R, Cremerius U, Büll U and Westhofen M. Results of pretherapeutic lymph node diagnosis in head and neck tumors. Clinical value of 18-FDG positron emission tomography (PET). Laryngorhinootologie 2000; 79: 201-6.

[11]   Pijl JP, Nienhuis PH, Kwee TC, Glaudemans AWJM, Slart RHJA and Gormsen LC. Limitations and pitfalls of FDG-PET/CT in infection and inflammation. Semin Nucl Med 2021; 51: 633-45.

[12]   Barnett CM, Sommerville RS, Lin C, Ratnayake G, Hughes B and Taheri T. CXCR4 and PD-1 expression in head and neck cancer with perineural spread. J Neurol Surg B Skull Base 2019; 80: 18-22.

[13]   Knopf A, Bahadori L, Fritsche K, Piontek G, Becker CC, Knolle P, Krüger A, Bier H and Li Y. Primary tumor-associated expression of CXCR4 predicts formation of local and systemic recurrency in head and neck squamous cell carcinoma. Oncotarget 2017; 8: 112739-47.

[14]   Lapa C, Herrmann K, Schirbel A, Hanscheid H, Luckerath K, Schottelius M, Kircher M, Werner RA, Schreder M, Samnick S, Kropf S, Knop S, Buck AK, Einsele H, Wester HJ and Kortüm KM. CXCR4-directed endoradiotherapy induces high response rates in extramedullary relapsed multiple myeloma. Theranostics 2017; 7: 1589-97.

[15]   Serfling SE, Zhi Y, Megerle F, Fassnacht M, Buck AK, Lapa C and Werner RA. Somatostatin receptor-directed molecular imaging for therapeutic decision-making in patients with medullary thyroid carcinoma. Endocrine 2022; 78: 169-76.

[16]   Kosmala A, Serfling SE, Schlötelburg W, Lindner T, Michalski K, Schirbel A, Higuchi T, Hartrampf PE, Buck AK, Weich A and Werner RA. Impact of 68 Ga-FAPI-04 PET/CT on staging and therapeutic management in patients with digestive system tumors. Clin Nucl Med 2023; 48: 35-42.

[17]   McCarty KS Jr, Szabo E, Flowers JL, Cox EB, Leight GS, Miller L, Konrath J, Soper JT, Budwit DA, Creasman WT, et al. Use of a monoclonal anti-estrogen receptor antibody in the immunohistochemical evaluation of human tumors. Cancer Res 1986; 46 Suppl: 4244s-4248s.

[18]   Mehanna H, Wong WL, McConkey CC, Rahman JK, Robinson M, Hartley AG, Nutting C, Powell N, Al-Booz H, Robinson M, Junor E, Rizwanullah M, von Zeidler SV, Wieshmann H, Hulme C, Smith AF, Hall P and Dunn J; PET-NECK Trial Management Group. PET-CT surveillance versus neck dissection in advanced head and neck cancer. N Engl J Med 2016; 374: 1444-54.

[19]   Smith AF, Hall PS, Hulme CT, Dunn JA, McConkey CC, Rahman JK, McCabe C and Mehanna H. Cost-effectiveness analysis of PET-CT-guided management for locally advanced head and neck cancer. Eur J Cancer 2017; 85: 6-14.

[20]   Linz C, Brands RC, Herterich T, Hartmann S, Muller-Richter U, Kubler AC, Haug L, Kertels O, Bley TA, Dierks A, Buck AK, Lapa C and Brumberg J. Accuracy of 18-F fluorodeoxyglucose positron emission tomographic/computed tomographic imaging in primary staging of squamous cell carcinoma of the oral cavity. JAMA Netw Open 2021; 4: e217083.

[21] Gu B, Xu X, Zhang J, Ou X, Xia Z, Guan Q, Hu S, Yang Z and Song S. The added value of (68) Ga-FAPI PET/CT in patients with head and neck cancer of unknown primary with (18) F-FDG-negative findings. J Nucl Med 2022; 63: 875-81.

[22] Ferdinandus J, Costa PF, Kessler L, Weber M, Hirmas N, Kostbade K, Bauer S, Schuler M, Ahrens M, Schildhaus HU, Rischpler C, Grafe H, Siveke JT, Herrmann K, Fendler WP and Hamacher R. Initial clinical experience with (90)Y-FAPI-46 radioligand therapy for advanced-stage solid tumors: a case series of 9 patients. J Nucl Med 2022; 63: 727-34.

[23] De-Colle C, Menegakis A, Monnich D, Welz S, Boeke S, Sipos B, Fend F, Mauz PS, Tinhofer I, Budach V, Abu Jawad J, Stuschke M, Balermpas P, Rödel C, Grosu AL, Abdollahi A, Debus J, Belka C, Ganswindt U, Pigorsch S, Combs SE, Lohaus F, Linge A, Krause M, Baumann M and Zips D; DKTK-ROG. SDF-1/CXCR4 expression is an independent negative prognostic biomarker in patients with head and neck cancer after primary radiochemotherapy. Radiother Oncol 2018; 126: 125-31.

[24] Buck AK, Haug A, Dreher N, Lambertini A, Higuchi T, Lapa C, Weich A, Pomper MG, Wester HJ, Zehndner A, Schirbel A, Samnick S, Hacker M, Pichler V, Hahner S, Fassnacht M, Einsele H, Serfling SE and Werner RA. Imaging of C-X-C motif chemokine receptor 4 expression in 690 patients with solid or hematologic neoplasms using (68)Ga-Pentixafor PET. J Nucl Med 2022; 63: 1687-92.

[25] Victora GD and Nussenzweig MC. Germinal centers. Annu Rev Immunol 2022; 40: 413-42.

[26] Allen CD, Ansel KM, Low C, Lesley R, Tamamura H, Fujii N and Cyster JG. Germinal center dark and light zone organization is mediated by CXCR4 and CXCR5. Nat Immunol 2004; 5: 943-52.

[27] Sivarajah S, Isaac A, Cooper T, Zhang H, Puttagunta L, Abele J, Biron V, Harris J, Seikaly H and O'Connell DA. Association of fludeoxyglucose F 18-labeled positron emission tomography and computed tomography with the detection of oropharyngeal cancer recurrence. JAMA Otolaryngol Head Neck Surg 2018; 144: 1037-43.

[28] Buck AK, Grigoleit GU, Kraus S, Schirbel A, Heinsch M, Dreher N, Higuchi T, Lapa C, Hänscheid H, Samnick S, Einsele H, Serfling SE and Werner RA. C-X-C motif chemokine receptor 4-targeted radioligand therapy in patients with advanced T-cell lymphoma. J Nucl Med 2023; 64: 34-9.

[29] Buck AK, Serfling SE, Kraus S, Samnick S, Dreher N, Higuchi T, Rasche L, Einsele H and Werner RA. Theranostics in hematooncology. J Nucl Med 2023; 64: 1009-16.